Bulletin KRASEC. Phys. & Math. Sci. 2016. V. 12. no. 1. pp. 58-74. ISSN 2313-0156

DOI: 10.18454/2313-0156-2016-12-1-58-74

MSC 86A10+86A25

ANALYSIS OF SPACE WEATHER EVENTS OF 2014 ACCORDING TO THE OBSERVATIONS IN THE NORTH-EASTERN REGION OF RUSSIA

S. E. Smirnov[1], V. V. Bychkov[1], O. V. Mandrikova[1], I. S. Solovev[1], Yu. A. Polozov[1], T. L. Zalyaev[1], S. Y. Khomutov[1], D. G. Baishev[2], I. N. Poddelsky[1], Z. F. Dumbrava[1]

[1] Institute of Cosmophysical Research and Radio Wave Propagation FEB RAS, 684034, Kamchatskiy Kray, Paratunka, Mirnaya st., 7, Russia

[2] Yu.G. Shafer Institute of Cosmophysical Research and Aeronomy SB RAS, 677980, Yakutsk, Lenin boul., 31, Russian

E-mail: sergey@ikir.ru

The paper considers geophysical effects of solar events of 2014 based the observation system of the north-eastern Russia. The effects of wave excitation were detected in atmospheric electricity of the near ground air which occurred in the result of a sudden commencement of a magnetic storm. Positive anomalies were observed in the ionosphere before the events on November 4, 2014 and August 27, 2014. They occurred at the background of calm and weakly disturbed geomagnetic field regardless of local time.

Key words: space weather, ionosphere, magnetic storm

Introduction

Complex analysis of space weather effects according to the observations of geophysical observatory network allows us to reveal the consequence and the complexity of the processes of geosphere shell interaction during extreme solar events. This paper considers the solar events of 2014.

Smirnov Sergey Eduardovich – Ph.D. (Phys. & Math.), Leading Researcher Systems Analysis Laboratory, Institute of Space Physics Research and Radio Wave Propagation FEB RAS.

Bychkov Vasilij Valentinovich – Ph.D. (Phys. & Math.), Team Leader sensing of the atmosphere and ionosphere, Institute of Space Physics Research and Radio Wave Propagation FEB RAS.

Mandrikova Oksana Viktorovna – D. (Tech.), Head of Head of the Systems Analysis Laboratory, Institute of Space Physics Research and Radio Wave Propagation FEB RAS.

Polozov Yuriy Aleksandrovich – Ph.D. (Tech.), Senior Researcher, Systems Analysis Laboratory, Institute of Space Physics Research and Radio Wave Propagation FEB RAS.

Zaljaev Timur Lenarovich – Junior Researcher Systems Analysis Laboratory, Institute of Space Physics Research and Radio Wave Propagation FEB RAS.

Khomutov Sergey Yur'evich – Ph.D. (Phys. & Math.), Head comprehensive geophysical observatory, Institute of Space Physics Research and Radio Wave Propagation FEB RAS.

Baishev Dmitrij Gavril'evich – Ph.D. (Phys. & Math.), Head of the Laboratory magnetosphere–ionosphere researches, Yu.G. Shafer Institute of Cosmophysical Research and Aeronomy SB RAS.

©Smirnov S. E., Bychkov V. V., Mandrikova O. V. et al, 2016.

Investigation of the character of the Earth magnetic field variation is the basis for estimation of electromagnetic field state and properties in the near space. In the result of solar wind impact on the Earth magnetosphere, the parameters of magnetic and electric field change as well as the parameters of current intensities and precipitating particle fluxes, different waves are excited [1]. All these values are used to estimate the strength of a magnetic storm characterizing solar effect on the near space.

One of the important tasks in the investigation of space weather is the control of ionosphere state and detection of anomalies [2]-[7]. Ionospheric parameters significantly change with height, depend on the cycle of the solar activity, geomagnetic conditions, geographic coordinates and contain characteristic diurnal and seasonal changes [2]-[5]. Ionospheric anomalies appear in the form of considerable deviation (increase or decrease) of electron concentration in relation to the background level. In most cases, ionospheric disturbances occur in the result of increased solar or geomagnetic activity and in seismically active regions they may also be observed during increased seismic activity [2]-[4],[8],[9].

Cosmic ray variations observed on the Earth surface are the integrated result of different solar, heliospheric and atmospheric phenomena and have a complex inner structure [10],[11]. Their intensity depends on weather parameters, in particular, on air temperature and pressure, geomagnetic field state, electromagnetic environment in the solar system and physical conditions in the Galaxy [10]-[12]. 11-year cycle and 27-day solar period of rotation reflect in space ray variations [11]. The variations also contain the diurnal changes determined by magnetospheric asymmetry which varies in time with the changes of solar wind parameters [13]. Owing to the complex structure of the recorded data, methods of wavelet transform and neural networks are applied in this work for the investigation. [14],[15].

Research of the effects of solar and geomagnetic activity on quasi-static electric field and weather parameters in the near ground atmosphere at high- and mid- latitudes has been carried out for comparatively short time. Many papers are devoted to this question [for example, [16],[17]]. The works which have been recently carried out are reviewed in the article [18], which shows the inconsistency of the obtained results and suggested mechanism of the observable effects. Earlier, we considered the effects of weak [19] and extreme [18] geomagnetic storms in the potential gradient (PG) variation. During small magnetic storms with gradual commencement, there are no cause-effect relations between PG variations and those of geomagnetic field horizontal component in "fair weather"conditions. During strong magnetic storms, the galactic cosmic rays reach the lower atmosphere and become the determinating factor of ionization of the near ground air.

In the paper [20] the authors describe an increase of air electrical conductivity within two days before the geomagnetic storm on October 29-30, 2003 caused by cosmic ray effect and its decrease during the Forbush-decrease of galactic cosmic rays accompanied by PG growth.

The general conclusion from these papers was that no matter if a storm is strong or weak, with gradual beginning and without any changes in air electrical conductivity, there are no significant changes in PG. This paper presents different solar events of 2014 including that with a sudden commencement. It was interesting to investigate the PG reaction on these events.

Observation system

Geophysical observatories (GO) and sites (GS) of IKFIA SB RAS and IKIR FEB RAS form an observation network in the north-eastern part of the Siberia and the Far East of Russia (see Table and Fig. 1).

Table

IKFIA and IKIR geophysical observatories and sites

		Geograph.		Geomag.							
Obs/Station	IAGA	latitude (N)	longitude (E)	latitude (N)	longitude (E)	M	E	I	C	L	Inst
Kotelny	KTN	76.00	137.90	66.98	198.39	+					1
Cape Schmidt	CPS	68.88	180.63	64.26	233.02	+			+		2
Chokurdakh	CHD	70.62	147.89	62.38	207.83	+					1
Tixie	TIK	71.60	128.80	62.19	194.34	+					1
Zyryanka	ZYK	65.75	150.78	57.86	212.18	+					1
Zhigansk	ZGN	66.80	123.40	57.19	191.58	+		+			1
Yakutsk	YAK	62.00	129.70	52.65	197.12	+		+			1
Magadan	MGD	60.05	150.73	52.25	214.18	+		+	+		2
Paratunka	PET	52.97	158.25	46.07	222.49	+	+	+		+	2
Khabarovsk	KHB	47.61	134.69	38.60	203.34	+		+			2

Notes: (a) geomagnetic coordinates were calculated for 2014 based on IGRF12 model (http://wdc.kugi.kyoto-u.ac.jp/igrf/gggm/index.html); (b) types of observatory measurements: M – geomagnetic field, E – atmospheric electricity, I – ionosphere, C – cosmic rays, L – lidar; (c) Inst – affiliation: 1 – IKFIA, 2 – IKIR.

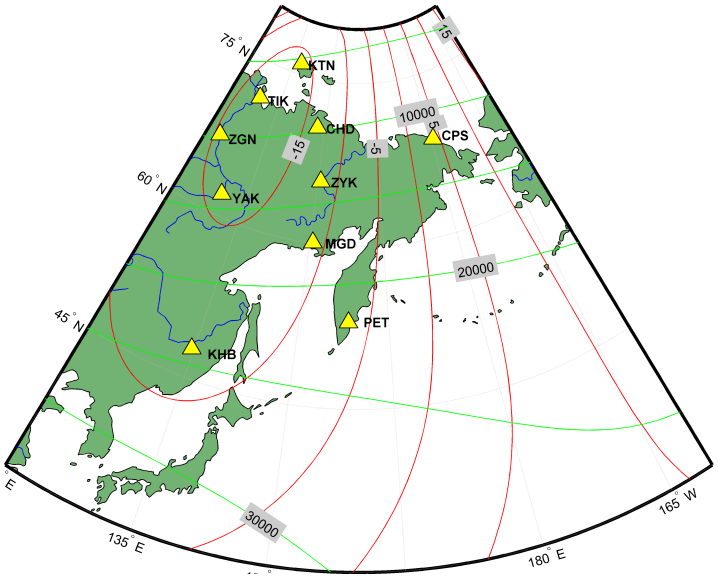

Fig. 1. Map of location of IKFIA and IKIR observatories. Declination and horizontal component of the magnetic field shown by the isolines were calculated by WMM2015 model (http://www.ngdc.noaa.gov/geomag/WMM/index.html)

Methods of investigation

Modeling of cosmic ray variation and detection of anomalous changes on the basis of combination of multi-scale wavelet decompositions and neural network. To analyze the cosmic ray variations, we used a neural network model suggested in the papers [14],[15]. The model is based on the joint application of multi-scale decompositions of time series and multilayer neural networks of direct transmission of a signal. The model is described below.

Based on multi-scale wavelet decompositions to the level of m, we obtained data representation in the form [21], [22]

$$f_0(t) = \sum_{j=-1}^{-m} f^d\left[2^j t\right] + f^a\left[2^{-mt}\right],$$

where $f^a\left[2^j t\right] \in W_j, f^a\left[2^{-m}t\right] \in V_{-m}$, $W_j = clos_{L^2(R)}\left(2^{j/2}\Psi\left(2^j t - n\right)\right) : n \in Z$, Φ is the basic wavelet; $V_j = clos_{L^2(R)}\left(2^{j/2}\phi\left(2^j t - n\right)\right) : n \in Z$, ϕ is the scaling function; j is resolution. The components of the series $f^a\left[2^{-m}t\right] = \sum c_{-m,n}\phi_{-m,n}(t)$, $c_{-m,n} =< f, \phi_{-m,n} >$, are smooth components. The components $f^d\left[2^j t\right] = \sum\limits_n d_{j,n}\Psi_{j,n}(t)$, where $d_{j,n} =< f, \Psi_{j,n} >$ are different-scale detailing components.

We applied wavelets of Coiflet family determined by minimization of approximation error [14]. For the components obtained after decomposition, wavelet reconstruction (for each component separately) was carried out

$$f_0(t) = f_0^{a(-m)}(t) + \sum_{j=-1}^{-m} f_0^{d,j}(t),$$

where $f_0^{a(-m)}(t) = \sum\limits_n c_{0,n}^{(-m)}\phi_{0,n}(t)$, $f_0^{d,j}(t) = \sum\limits_n d_{0,n}^j \Psi_{0,n}(t)$, the superscrips $(-m), j$ correspond to the resolution of the component before wavelet reconstruction. Then, based on a neural network, we obtained a mapping for the smoothed component

$$y : f_0^{a(-m)} \longrightarrow f_0^{*a(-m)},$$

in which if $\hat{f}_0^{a(-m)}$ is a network actual output and $f_0^{*a(-m)}$ is a desirable one, then $f_0^{*a(-m)} = f_0^{a(-m)}$ is an unknown function and $\hat{f}_0^{*a(-m)}$ is its approximation which the neural network reconstructs.

The network error is determined as a difference between the desirable $f_0^{*a(-m)} = f_0^{a(-m)}$ and the actual $\hat{f}_0^{*a(-m)}$ output values of the function.

The algorithm of construction of a neural network and selection of the decomposition level is described in the papers [14], [15]. The model obtained by this algorithm and applied in this paper is the following:

$$c_{j,n+1}(t) = \varphi_m^3\left(\sum_i \omega_{mi}^3 \varphi_i^2\left(\sum_i \omega_{ii}^2 \varphi_i^1\left(\sum_n \omega_{1n}^1 c_{j,n}(t)\right)\right)\right),$$

where $c_{j,n} =< y, \phi_{j,n} >$, $\phi_{j,n}(t) = 2^{j/2}\phi\left(2^j t - n\right)$ is the scaling function, ω_{1n}^1 are neuron weight coefficients l of the network input layer, ω_{ii}^2 neuron weight coefficients i of the network hidden layer, ω_{ii}^3 neuron weight coefficients m of the output layer, $\varphi_i^1(z) = \varphi_i^2(z) = \dfrac{2}{1+\exp(-2z)} - 1, \varphi_m^3(z) = az + b$. The coefficients $c_{j,n}$ are the result of mapping of the initial function y into a space of scale j.

Detection of geomagnetic disturbances and estimation of their intensity. We used the presentation of geomagnetic field H-component suggested in the papers [14],[15] which has the form

$$f_0(t) = \sum_n c_{-m,n}\varphi_{-m,n}(t) + \sum_{j\in I}\sum_n d_{j,n}\Psi_{j,n}(t) + \sum_{j\notin I}\sum_n d_{j,n}\Psi_{j,n}(t) = f_{trend}(t) + f_{\text{возмущ}}(t) + e(t).$$

where the component of the model $f_{trend}(t) = \sum_n c_{-6,n}\varphi_{-6,n}(t)$ describes undisturbed level of the Earth magnetic field horizontal component during calm periods and the component $f_{\text{возмущ}}(t) = \sum_{j\in I} g_j(t)$ where $g_j(t) = \sum_n d_{j,n}\Psi_{j,n}(t)$ describes geomagnetic disturbances. The component $e(t) = \sum_{j\notin I}\sum_n d_{j,n}\Psi_{j,n}(t)$ is a noise one, I is a set of indexes. As a measure of magnetic disturbance of the component $g_j(t)$ on the scale j, we applied the value $A_j = \max_n(|d_{j,n}|)$ [14], [15]. The set of indexes was determined based on the criteria

$$j \in I, \text{если } m\left(A_j^v\right) > m\left(A_j^k\right) + \varepsilon,$$

where m is a sample average, v is the index of field disturbed variation, k is the index of field calm variation, ε is some positive number.

Taking into account the equivalence of discrete and continuous wavelet transformations [21], [22] determined as

$$W_\Psi f_{b,a} := |a|^{-1/2}\int_{-\infty}^{\infty} f(t)\,\Psi\left(\frac{t-b}{b}\right)dt, f \in L^2(R), a, b \in R, a \neq 0.$$

and according to the measure of coefficient magnetic disturbance mentioned above, the intensity of geomagnetic disturbances at a time point $t = b$ on the scale under analysis was estimated using the value

$$e_{a,b} = |W_\Psi f_{b,a}|.$$

Then the field disturbance intensity at a time moment $t = b$ is

$$E_b = \sum_a e_{b,a}.$$

Detection of anomalies in the ionosphere and estimation of their parameters on the basis of continuous wavelet transform Amplitude decrease of the coeffiecients $|W_\Psi f_{b,a}|$ in relation to the scale a is associated with proportional and point smoothness of Lipschitz function f [21], [23]. When the scale a decreases, amplitudes of the coefficients $|W_\Psi f_{b,a}|$ decrease fast to zero in the domains where function f does not have local peculiarities [23], [24]. Based on this property of wavelet transform, in order to detect anomalous features in ionospheric critical frequency parameters, we used the threshold function

$$P_{T_0}(W_\Psi f_{b,a}) = \begin{cases} W_\Psi f_{b,a}, \text{если } |W_\Psi f_{b,a} - W_\Psi f_{b,a}^{med}| \geq T_a \\ 0, \text{если } |W_\Psi f_{b,a} - W_\Psi f_{b,a}^{med}| < T_a, \end{cases}$$

where the threshold $T_a = U * St_a$ determines the presence of an anomaly on the scale a near the point ξ contained in the carrier $\Psi_{b,a}$, $St_a = \sqrt{\frac{1}{\Phi-1}\sum_{k=1}^{\Phi}\left(W_\Psi f_{b,a} - \overline{W_\Psi f_{b,a}}\right)^2}$, $\overline{W_\Psi f_{b,a}}$ и $W_\Psi f_{b,a}$ are the average value and the median determined separately for each hour in a moving time window with the length of Φ, U is a threshold coefficient.

To estimate the threshold coefficient U, a posterior risk was used in the paper [25]. The state of the ionosphere was determined by ionograms which were also compared with geomagnetic data (K index was used). In terms of the solar cycle, the thresholds for the year periods with high and low solar activity were estimated separately.

When the wavelet Ψ has a compact carrier equal to $[-\Omega, \Omega]$, a set of point pairs (b, a) such that the point ξ is contained in the carrier $\Psi_{b,a}$ determine the cone of influence of the point ξ. As long as the carrier $\Psi_{b,a}$ on the scale a is equal to $[b-\Omega a, b+\Omega a]$, the cone of influence of the point ξ on the scale a is determined by the inequality

$$|b - \xi| \leq \Omega a.$$

Thus, the duration of an anomaly on the scale a is determined by the cone of influence of the point xi and equals

$$H_a = 2\Omega a.$$

Anomaly intensity at a time point $t = b$ was calculated as

$$I_b = \sum_a |P_{T_0}(W_\Psi f_{b,a})|.$$

Events on August 27-30, 2014

A geomagnetic storm with gradual commencement was recorded at "Paratunka (PET) and "Magadan"observatories on August 27, 2014 from 09:45 to 10:15 UT. Solar wind velocity increased from 300 to 480 km/s on August 27-29 in the result of arrival of accelerated flux from coronal mass ejection (CME on August 25) and from recurrent coronal hole (http://ipg.geospace.ru /space-weather-review-20-08-2014.html). The results of modeling of cosmic ray variations show that insignificant local oscillations relatively the background level were observed before the storm on August 26. Neural network error had local increases. Geomagnetic disturbances at PET observatory were the most intensive on August 27 from 10:00 to 10:30 UT and from 18:00 to 19:00 UT (Fig. 2d).

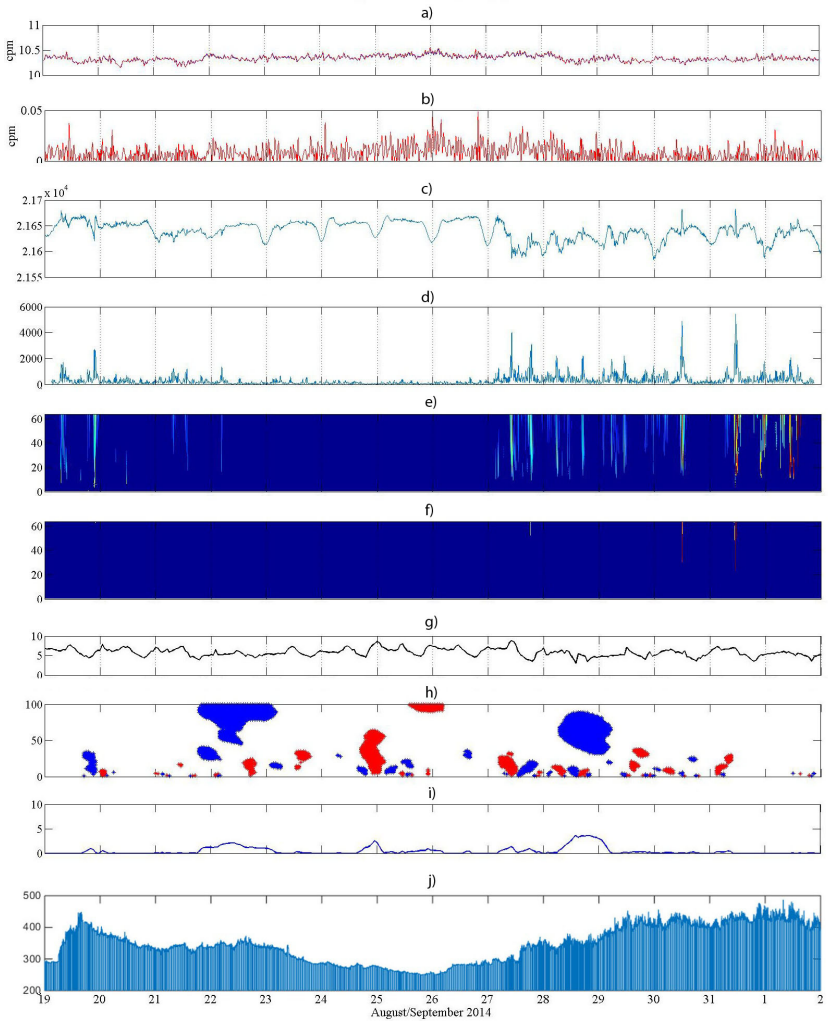

Fig. 2. Results of data processing for the period from August 19 to September 1, 2014.

Fig. 2 shows: a) – a5 component of neutron monitor signal and its approximation by neural network, MGD observatory; b) – neural network error; c) – H-component of the Earth magnetic field, PET observatory; d) – estimate of geomagnetic disturbance intensities; e) – detection of periods of weak and strong geomagnetic disturbances; f) – detection of periods of strong geomagnetic disturbances; g) – foF2 data, PET observatory; h) – detection of anomaly, threshold coefficient $U = 2.5$, length of a moving time window is $\Phi = 336$ hours; i) – estimate of anomaly intensity; j) – solar wind velocity.

According to the results of processing of ionospheric parameters, an increase of electron concentration was observed in the region of Kamchatka by day LT on August 25 during the coronal mass ejection. A positive ionospheric anomaly was also formed during that time which lasted for about 4-5 hours (Fig. 2h red color).

During the geomagnetic storm on August 28, the electron concentration significantly decreased in the ionosphere as evidenced by a large-scale negative anomaly with about one day duration which reached its intensity at nighttime LT (Fig. 2h blue color).

During the geomagnetic disturbance on August 28-30, 2014, the lidar sounding of the atmosphere at the wavelength of 532 nm was not carried out on August 29 and 30 owing to the weather conditions. According to PET observatory data, nighttime corpuscular Es were recorded on those days.

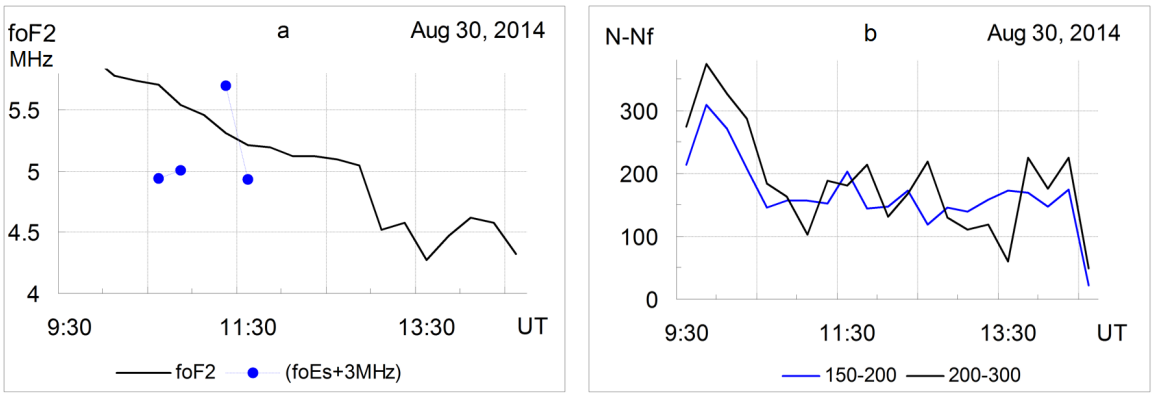

Fig. 3. The critical frequency of ionospheric F2 layer (a) and lidar signal from the heights of 150-200 and 200-300 km (b) during the geomagnetic disturbance on August 30, 2014

Fig 3a,b illustrates the results of observations on August 30. Dots in Fig. 3a show foEs values. For convenience in mapping them on one graph with foF2, all foEs values are increased by 3 MHz.

Increase of nighttime foF2 values is observed within the intervals 11:15 – 13:15 and 13:45 – 14:15 UT as well as the increase of the lidar total signal from the heights of 150-200 and 200-300 km within the same intervals of time. Nighttime corpuscular Es occurred at the heights of 100-114 km. Total signals from the layers of 150-200 and 200-300 km have the correlation coefficient among themselves equal to 0.78.

Correlated behavior of lidar signals from different layers is not characteristic for the heights of more than 100 km. Such behavior of a lidar signal may be explained by the resonance scattering at excited ions of nitrogen atom in the region of 150-300 km during electron precipitations into the ionosphere [26].

On August 27 and 28 the electric field of the near ground atmosphere had a typical diurnal variation in fair weather conditions at PET observatory [27]. This variation has two maxima within the day (Fig.4).

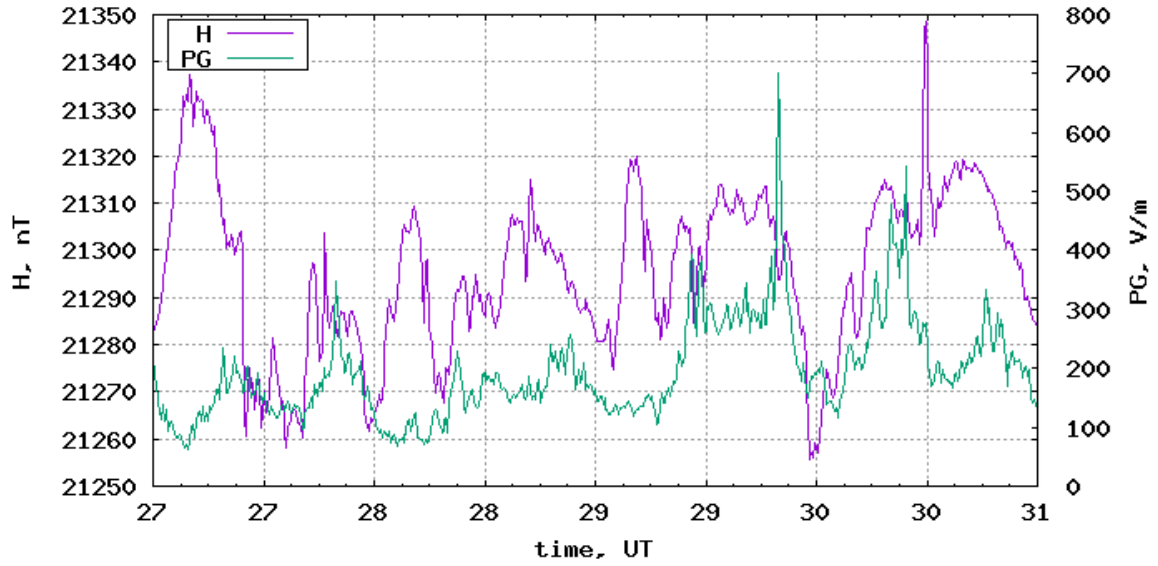

Fig. 4. Variations of magnetic field H-component (left scale) and of potential gradient (right scale) in the near ground atmosphere on August 27-30, 2014, PET observatory

The main maximum occurs during the sunrise and is determined by morning convective generator. The second one occurs during the evening and is associated with local decrease of air electrical conductivity. Local time of the site is shifted by 12 hours relatively the universal time, thus the main maximum occurs at the end of the day according to UTC. In spite of fair weather conditions, on August 29 the diurnal variation is disturbed and a deep minimum coincides with the main phase of the magnetic storm.

Events on September 12-13, 2014.

The geomagnetic storm with gradual commencement on September 11, 2014 was recorded at PET and MGD observatories at 23:30. Half an hour before the storm, at 23:02 UT, the solar wind velocity rapidly increased from v=350 km/s to 480 km/s in the result of accelerated flux from a coronal ejection (CME on September 9 from the flare M4.5/1N)(http://ipg.geospace.ru/space-weather-review-10-09-2014.html). On the next day, September 12, the solar wind velocity increased to 670 km/s at 15:27 UT due to the accelerated flux from the coronal ejection (CME on September 10 from the flare X1.6/2B), then it became v=800 km/s by the end of the day (http://ipg.geospace.ru/space-weather-review-10-09-2014.html). Based on the results of magnetic data processing from PET observatory, local increase of geomagnetic activity was observed before the magnetic storm on September 11 from 03:15 to 03:40. Maximum increases of geomagnetic disturbances in the region under analysis were observed on September 12, 2014 from 15:45 to 16:50 and from 20:30 to 23:30 UT.

Fig. 5 shows: a) – a5 component of neutron monitor signal and its approximation by neural network, MGD observatory; b) – a5 component of neutron monitor signal and its approximation by neural network, CPS observatory; c) – neural network error, MGD observatory; d) – neural network error, CPS observatory; e) – H-component of the Earth magnetic field, PET observatory; f) – estimate of geomagnetic disturbance intensities; g) – detection of periods of weak and strong geomagnetic disturbances; h) – detection of periods of strong geomagnetic disturbances; i) – foF2 data, PET observatory; j) – detection of anomaly, threshold coefficient is $U = 2.5$, length

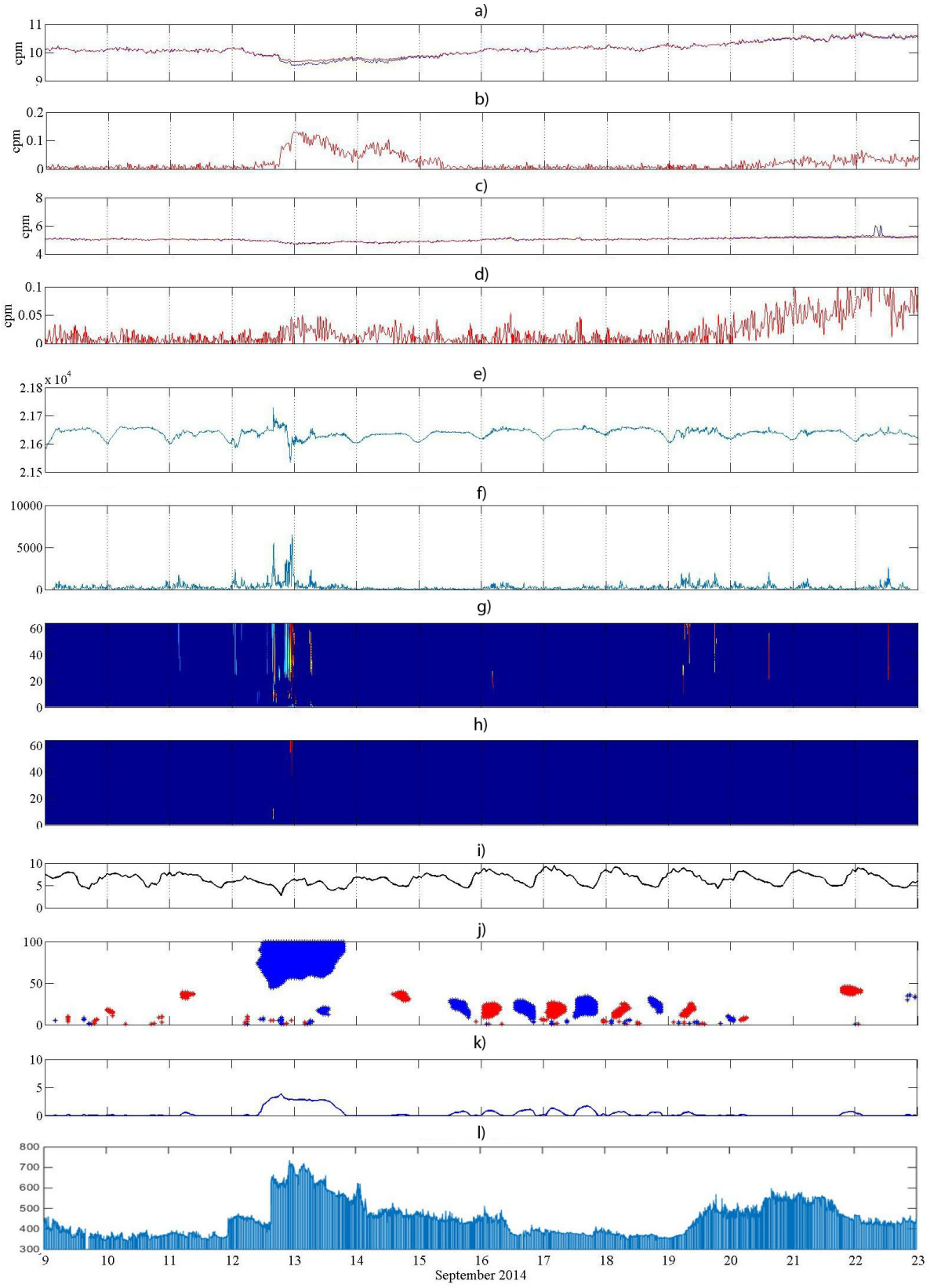

Fig. 5. Results of data processing for the period from September 9 to September 22, 2014.

of a moving time window is $\Phi = 336$ hours; k) – estimate of anomaly intensity; l) – solar wind velocity.

During the storm, a large-scale negative anomaly was formed in the ionosphere in the result of electron concentration decrease. It lasted for about a day and a half (Fig. 5j blue color).

Analysis of space variations shows that after the local decrease of the solar wind velocity, their level decreased and two Forbush-effects appeared, each of them lasted for about a day.

Coronal mass ejections occurred on September 15, 17, 18 and 19 (http://ipg.geospace.ru/-space-weather-review-10-09-2014.html). They caused the increase of the solar wind velocity from 350 to 560 km/s in the middle of the day on September 19.

During the coronal mass ejections (September 15, 17 and 18) electron concentration fluctuations occurred as evidenced by small-scale anomalies formed within this period (Fig. 5j,k).

Increase of geomagnetic disturbance intensity was recorded at PET observatory at 05:30 on September 19, 2014 (Fig. 5f,g,h).

According to cosmic ray data for the period of increase of solar wind velocity, a long Forbush-effect occurred on September 20. It was more clearly defined at CPS site (Fig. 5a,b,c,d).

During the storm on September 12-13, the lidar observations were carried out on September 12. The Moon phase was 88%, the culmination height was 44 degrees. High level of background signal and significant variations of foF2 values were observed. In such conditions, no lidar signals were recorded from the region of the upper atmosphere.

According to the data of ionospheric observations of PET observatory, corpuscular Es layer with the frequencies of 1.5-2.5 MHz was observed at the heights of 100-130 km on the both days as confirmed by the precipitations of electrons with the energies of hundreds of eV-units of keV into the atmosphere of Kamchatka. On September 12, the lidar observations were not carried out due to weather conditions.

On September 12, the electric field of the near ground atmosphere had a typical diurnal variation in fair weather conditions.

On September 13, the weather was cloudy, the diurnal variation was disturbed. No significant changes were observed in the electric field after the beginning of the magnetic storm (Fig.6).

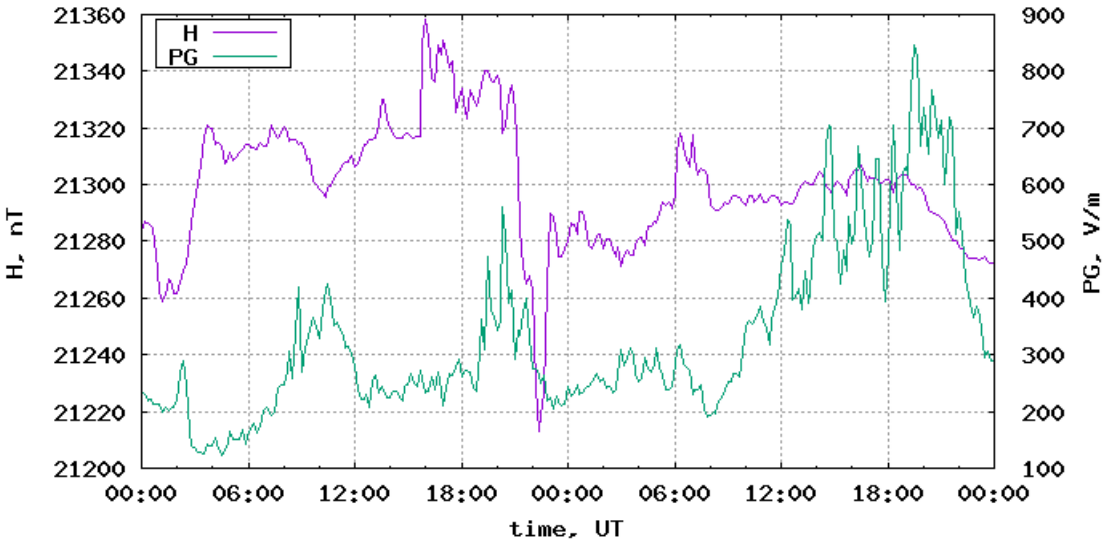

Fig. 6. Variations of magnetic field H-component (left scale) and potential gradient (right scale) in the near ground atmosphere on September 12-13, 2014, PET observatory

Events on November 4-5, 2014.

A magnetic storm was recorded at PET and MGD observatories on November 4, 2014 at 10:10 UT. Solar wind velocity from October 31 to November 1 increased from 300 km/s to 550 km/s due to the intersection of a sector boundary of MMF, activation of coronal filament in SE-quadrant of the disk and coronal mass ejections (http://ipg.geospace.ru/space-weather-review-29-10-2014.html). One day before the magnetic storm, on November 3, insignificant increase of electron concentration in the ionosphere was observed at PET observatory. A positive anomaly was also formed. It lasted for about one day and a half (Fig. 7d red colour).

On the next day, November 4, the solar wind velocity increased from 400 to 490 km/s under the effect of accelerated fluxes of the coronal hole and coronal mass ejection (CME on November 4) (http://ipg.geospace.ru/space-weather-review-29-10-2014.html). During this period, geomagnetic disturbances increased in the region of Kamchatka and reach the highest intensity from 11:00 to 15:00 UT (Fig. 7h). Some hours later, electron concentration in the ionosphere decreased considerably and a positive anomaly was changed by a negative one reaching the highest intensity during the main phase of the geomagnetic storm mainly by day LT (Fig. 7d blue colour).

The results of modeling of cosmic ray variations indicate local fluctuations of the level and a sequence of short Forbush-effects which occurred at the times of formation of the positive ionospheric anomaly on November 3 and were the most intensive during the significant increase of geomagnetic activity and formation of the negative large-scale anomaly in the ionosphere. Short-term recovery of cosmic ray level occurred only on November 9. On the next day, November 10, their level decreased simultaneously with the increase of geomagnetic activity.

Fig. 7 shows: a) – neutron monitor signal, MGD observatory; b) – neuron network error; c) – H-component of the Earth magnetic field, PET observatory; d) – detection of periods of weak and strong geomagnetic disturbances; e) – estimation of geomagnetic disturbance intensities; f) – foF2 data, PET observatory; g) – detection of an anomaly, threshold coefficient is $U = 2.5$, the length of a moving time window is $\Phi = 336$ hours; h) – estimate of anomaly intensities; i) – solar wind velocity.

During the geomagnetic disturbance on November 1-4, lidar observations were not carried out due to weather conditions. At nighttime on November 1-2, Es with the frequency of 2-2.5 MHz, including those of corpuscular type, occurred at the heights of about 100 km.

On November 3, nighttime Es occurred within 6:30-7:00 UT and 13:00-15:00 UT at the heights of about 100 km. Owing to the poor quality of ionograms, it is impossible to determine unambiguously the type of the layers.

On November 4, Es with the frequency of 2-2.5 MHz were observed from 7:15 to 9:30 and from 14:00 to 16:00 UT at the heights of 100-120 km. The type of the layers is corpuscular and one may talk on the presence of electron precipitations into the atmosphere early at night and at dawn.

On November 1-6, the electric field of the near ground atmosphere was determined by bad weather with heavy precipitation (Fig.8).

Events on December 23, 2014.

A magnetic storm was recorded at PET observatory on December 23 at 11:25 UT. Sudden increases of the solar wind velocity were observed from the end of the day on December 21 to the middle of the day on December 23. They were accompanied by weak disturbances of geomagnetic field.

According to the data of cosmic rays of MGD observatory, a long Forbush-effect was formed at the end of the day on December 21. The largest deviations of the variations relatively the typical level were observed during the geomagnetic storm on December 23 and 24.

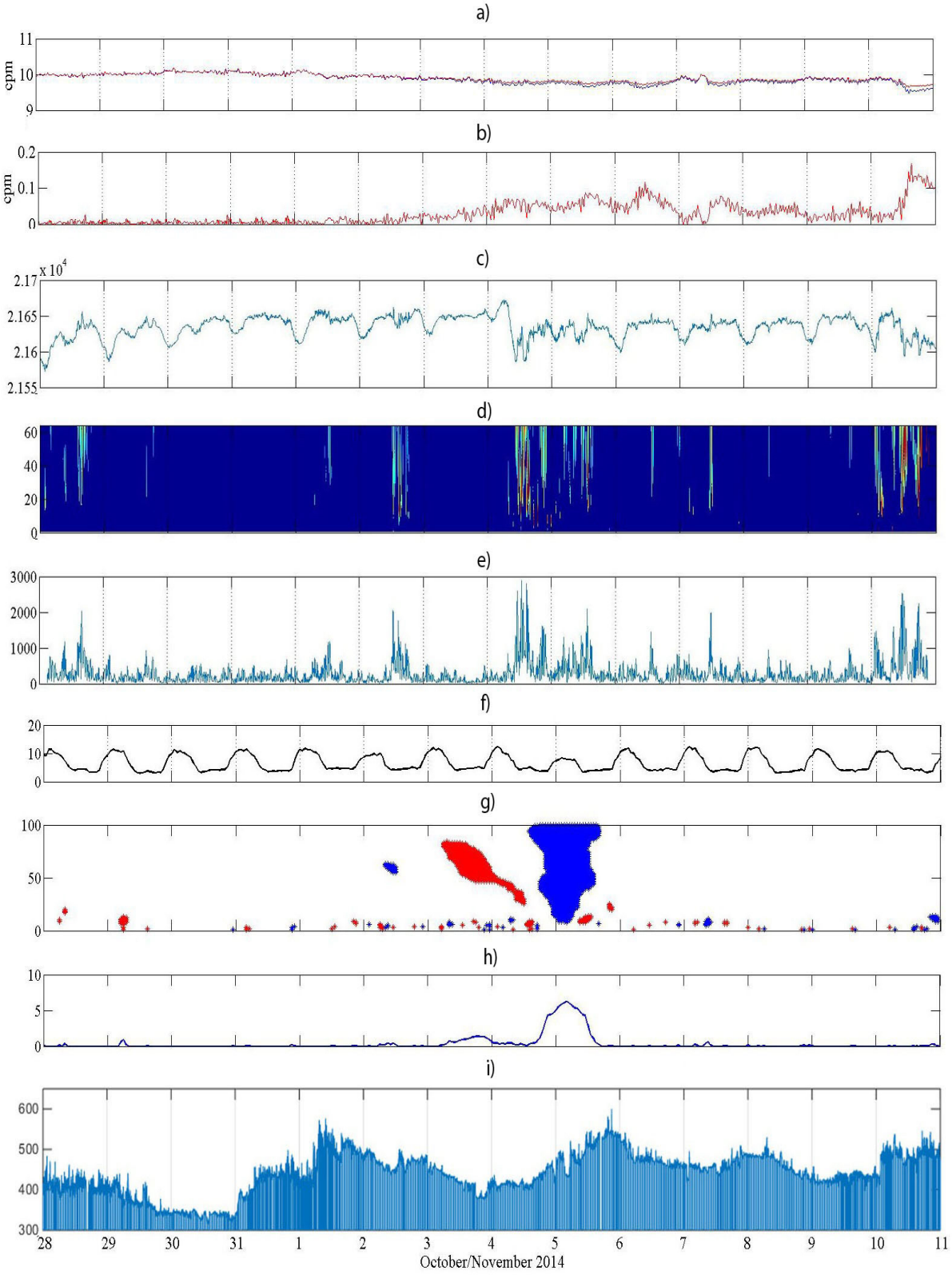

Fig. 7. Results of data processing for the period from October 28 to November 10, 2014.

During the same period of time, the electron concentration in the ionosphere in the region of Yakutsk significantly decreased and a large-scale negative anomaly was formed. It lasted for about a day and reached its highest intensity mainly by day LT (Fig. 9g blue colour).

Fig. 8. Variations of magnetic field H-component (left scale) and potential gradient (right scale) in the near ground atmosphere on November 1-5, 2014, PET observatory

Fig. 9 shows: a) – a5 component of neutron monitor signal and its approximation by neural network, MGD observatory; b) – neural network error; c) – H-component of the Earth magnetic field, PET observatory; d) – estimate of geomagnetic disturbance intensities; e) – detection of the periods of weak geomagnetic disturbances; f) – foF2 data, YAK observatory; g) – detection of anomaly, the threshold coefficient is $U = 2.5$, the length of a moving time window is $\Phi = 168$ hours; h) – estimate of anomaly intensities; i) – solar wind velocity.

On December 23, fair weather conditions were observed at PET observatory. The electric field of the near ground atmosphere before the magnetic storm had a decreased background. After a sudden commencement of the magnetic storm, a damping oscillating process with the period of ~ 1 hour began (Fig. 10). There were not any significant changes in the electrical conductivity of the near ground air. Similar reaction of PG on a magnetic storm with a sudden commencement was observed on April 5, 2010 [28].

Discussion of the results and conclusions

The most intensive geomagnetic disturbances occurred during significant increases of the solar wind velocity. Electron concentration in the ionosphere significantly decreased and large-scale negative anomalies were formed during the events under analysis.

Local fluctuations of the level of cosmic ray variations were recorded (short and long Frobush-effects). They were the most intensive during considerable increases of geomagnetic activity and formation of large-scale negative anomalies in the ionosphere. Similar effects were observed during the events on September 5, 2012 [15]. Before the beginning of the geomagnetic storms on November 4, 2014 and August 27, 2014, periods of anomalous decrease (relatively the background) of electron concentration in the ionosphere were detected at the background of calm and weakly disturbed geomagnetic field. They lasted from several hours to a day and a half.

In the paeprs [5], [6], similar pre-storm increases were observed at many ionospheric sites in different latitudinal and longitudinal zones. The questions associated with the mechanism and the source of this effect are still open.

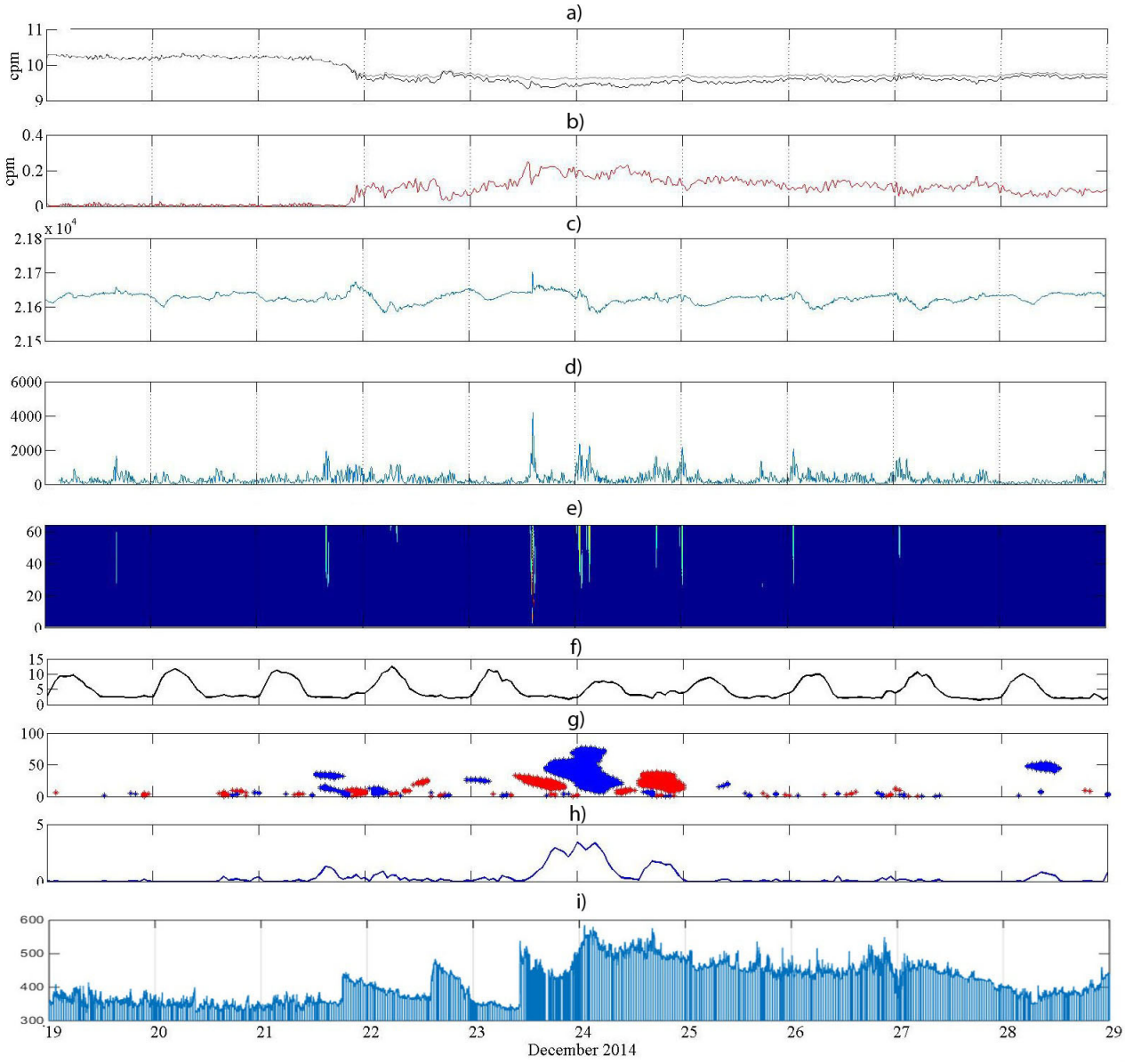

Fig. 9. Results of processing of the data for the period from December 19 to December 28, 2014.

It is interesting to consider the effect of the magnetic storm on December 23, 2014 on PG. The sudden commencement of the magnetic storm caused large fluctuations in PG with the period of ~ 1 hour at the mid-latitudinal observatory Paratunka with fast damping. The authors [29] suggest three mechanisms how a great solar storm may affect the atmospheric electricity.

The first one is atmosphere ionization by cosmic rays to the level of the Earth surface.

The second one is when a solar flare produces low-energy particles which enter the atmosphere but do not reach the Earth surface. In these conditions, the global electric circuit will be intensified due to the decrease of air resistance in the upper layers of the atmosphere that increases the conduction current between the ionosphere and the Earth surface which, in its turn, increases the PG.

The third mechanism comes from the increase of lightning activity by solar energy particles which could cause the increase of the current in the global circuit. There was no ionization by cosmic rays at that moment as long as there were no significant changes in air electrical

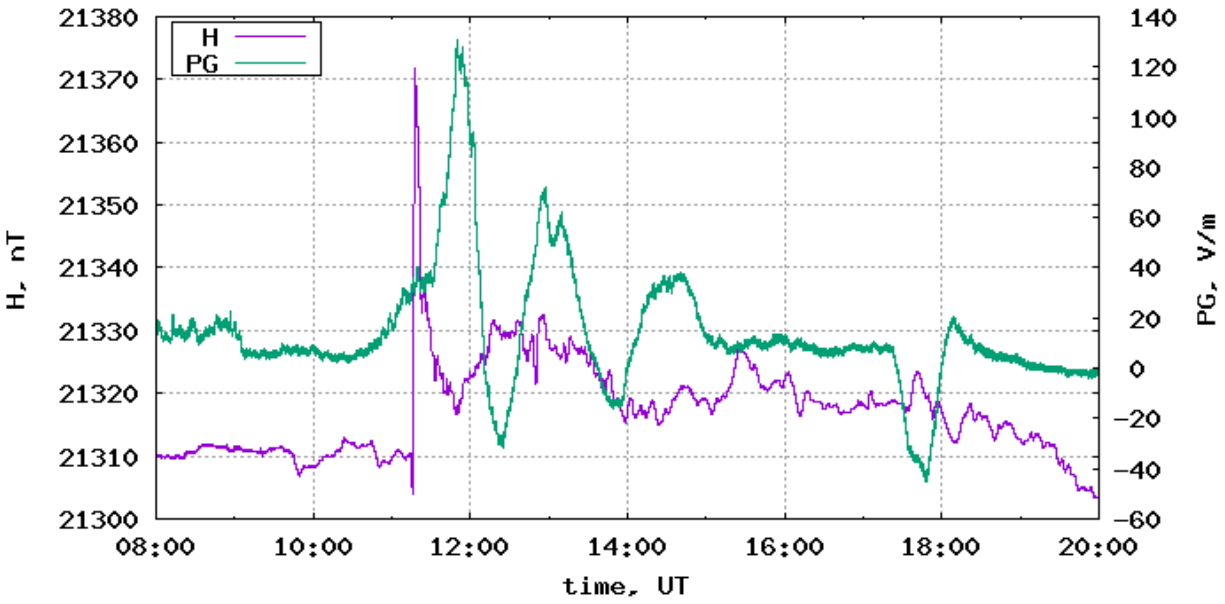

Fig. 10. Variations of magnetic field H-component (left scale) and of potential gradient (right scale) in the near ground atmosphere on December 23, 2014, PET observatory

conductivity. The third mechanism would cause a global effect at other sites which was not observed. The second mechanism is quite possible. However, other explanations of this effect are also possible. The fact that calls the attention is that large fluctuations in PG are caused not by high intensity of the magnetic storm but by a sudden front of its commencement. In comparison to that, strong storms with gradual commencement did not affect the PG of the near ground layer of the atmosphere. It was mentioned in the paper [18]. A similar effect was observed during a storm on April 5, 2010. In that case, during a sudden commencement, a large increase of PG was observed. As long as this process has a rapidly damping character, fluctuations did not manifest themselves [28].

Analysis of space weather based on the events of 2014 observed in the north-eastern region of Russia discovered the following effects:

1) during the solar flares, small-scale ionospheric anomalies, mainly positive and having different intensities, were discovered;

2) geomagnetic disturbances with the highest intensities occurred during significant increases of the solar wind velocity;

3) during the main phases of geomagnetic storms, electron density in the ionosphere significantly decreased and large negative anomalies were formed;

4) large-scale positive anomalies were distinguished in the ionosphere; they occurred before the beginning of the geomagnetic storms and lasted for one day and more;

5) local fluctuations of cosmic ray variations (Forbush-effect) were detected; they reached the highest intensities during significant increases of geomagnetic activity and when large-scale negative ionospheric anomalies were formed;

6) sudden commencement of the geomagnetic storm caused excitation of oscillation processes in the atmospheric electricity.

The authors are grateful to the staff of IKFIA and IKIR observatories and sites for qualitative measurements. The paper was supported by RSF Grant No. 14-11-00194, RF President Grant SP-2976.2013.

References

1. Akasofu S. I., Chapman S. Solar-Terrestrial Physics. Oxford. Oxford University Press. 1972. 891 p.

2. Afraimovich E., Kosogorov E., Palamarchouk K., Perevalova N., Plotnikov N. The use of GPS arrays in detecting the ionospheric response during rocket launchings. Earth, Planets and Space. 2000. vol. 52. no. 11. pp. 1066–1061

3. Afraimovich E., Perevalova N., Plotnikov A., Uralov A. The shock-acoustic waves generated by earthquakes. Ann. Geophys. 2001. vol. 19. no. 4. pp. 409–395. http://dx.doi.org/10.5194/angeo-19-395-2001

4. Nakamura M., Maruyama T., Shidama Y. 3-3-4 Using a Neural Network to Make Operational Forecasts of Ionospheric Variations and Storms at Kokubunji, Japan. Journal of the National Institute of Information and Communications Technology. 2009. vol. 56. no. 1–4. pp. 391–406

5. Danilov A. D. Ionospheric F-region response to geomagnetic disturbances. Advances in Space Research. 2013. vol. 52. no. 3. pp. 343–366

6. Liu L., Wan W., Zhang M. L., Zhao B. Case study on total electron content enhancements at low latitudes during low geomagnetic activities before the storms. Ann. Geophys. 2008. vol. 26. no 4. pp. 893–903.

7. Zhao X., Ning B., Liu L., Song G. A prediction model of short-term ionospheric foF2 based on AdaBoost. Advances in Space Research. 2014. vol. 53. no. 3. pp. 387–394

8. Klimenko M. V., Klimenko V. V., Zakharenkova I. E., Karpov I. V. Modeling of local disturbance formation in the ionosphere electron concentration before strong earthquakes. Earth, Planets and Space. 2012. vol. 64. no. 6. pp. 441–450

9. Klimenko M. V., Klimenko V. V., Ratovsky K. G., Goncharenko L. P. Numerical modeling of the global ionospheric effects of storm sequence on September 9-14, 2005 - comparison with IRI model. Earth, Planets and Space. 2012. vol. 64. no. 6. pp. 433–440

10. Toptygin I. N. Cosmic rays in interplanetary magnetic fields. Reidel Publ. Co. Dordrecht. 1985. 301 p.

11. Tyasto M. I., Danilova O. A., Dvornikov V. M., Sdobnov V. E. Bol'shie snizheniya geomagnitnykh porogov kosmicheskikh luchey v period sil'nykh vozmushcheniy magnitosfery [Large decreases of geomagnetic thresholds of cosmic rays during strong disturbances of the magnetosphere]. Izvestiya Rossiyskoy akademii nauk. Seriya Fizicheskaya – Bulletin of the Russian Academy of Sciences. Physics. 2009. vol. 73. no. 3. pp. 385–388

12. Gopalswamy N., Xie H., Yashiro S., Usoskin I. Ground level enhancement events of Solar cycle 23. Indian Journal of Radio & Space Physics. 2010. vol. 39. pp. 240–248

13. Kota J., Somogyi A. Some problems of investigating periodicities of cosmic ray time series. Acta Physica Academiae Scientiarum Hungaricae. 1969. vol. 27. no. 1–4. pp. 523–548

14. Mandrikova O. V., Solovjev I., Geppenerc V., Taha Al-Kasasbehd R., Klionskiy D. Analysis of the Earth's magnetic field variations on the basis of a wavelet-based approach. Digital Signal Processing. 2013. vol. 23. no. I.1 pp. 329–339

15. Mandrikova O. V., Solovjev I. S, Zalyaev T. L. Methods of analysis of geomagnetic field variations and cosmic ray data. Earth, Planets and Space. 2014. vol. 66. no. 1. http://dx.doi.org/10.1186/s40623-014-0148-0

16. Paramonov N. A. Atmosfernoe elektrichestvo [Atmospheric electricity]. Leningrad Gidrometeoizdat. 1969. 129 p.

17. Roble R. G. On solar-terrestrial relationships in atmospheric electricity. J. Geophys. Res. 1985. vol. 90. no. D4. pp. 6000–6012

18. Smirnov S. E., Mikhailova G. A., Kapustina O. V. Variations in the quasi-static electric field in the near-Earth's atmosphere during geomagnetic storms in November 2004. Geomagnetism and Aeronomy. 2013. vol. 54. no. 4. pp. 532–545 http://dx.doi.org/10.1134/S0016793213040130

19. Mikhailova G. A., Mikhailov Yu. M., Kapustina O. V., Druzhin G. I., Smirnov S. E. Power spectra of thermal tidal and planetary waves in the near-Earth atmosphere and in the ionospheric D region at Kamchatka. Geomagnetism and Aeronomy. 2009. vol. 49. no. 5. pp. 610–623. http://dx.doi.org/10.1134/S0016793209050089

20. Smirnov S. E., Mikhailova G. A., Kapustina O. V. Variations in electric and meteorological parameters in the near-Earth's atmosphere at Kamchatka during the solar events in October 2003. Geomagnetism and Aeronomy. 2014. vol. 54. no. 2 pp. 240–247. http://dx.doi.org/10.1134/S0016793214020182

21. Daubechies I. Ten Lectures on Wavelets. Philadelphia. SIAM. 1992. 357 p.

22. Chui C. K. An introduction in wavelets. New York. Academic Press. 1992. 264 p.

23. Mallat S. A Wavelet Tour of Signal Processing, Third Edition: The Sparse Way. Academic Press. 1999. 832 p.

24. Jaffard S. Pointwise smoothness, two-microlocalisation and wavelet coefficients. Publications Mathematiques.1991. vol. 35. pp.155–168

25. Levin B. R. Teoreticheskie osnovy statisticheskoy radiotekhniki [Theoretical bases of statistical radio engineering]. Moscow. Fizmatgiz. 1963. 1504 p.

26. Bychkov V. V., Nepomnyashchiy Y. A., Perezhogin A. S., Shevtsov B. M. Lidar returns from the upper atmosphere of Kamchatka for 2008 to 2014 observations. Earth, Planets and Space. 2014. vol. 66. no. 1. pp. 1–4. http://dx.doi.org/10.1186/s40623-014-0150-6

27. Smirnov S. E. Influence of a convective generator on the diurnal behavior of the electric field strength in the near-Earth atmosphere in Kamchatka. Geomagnetism and Aeronomy. 2013. vol. 53. no. 4. pp. 546–552. http://dx.doi.org/10.1134/S0016793213040142

28. Smirnov S. E. Reaction of electric and meteorological states of the near-ground atmosphere during a geomagnetic storm on 5 April 2010. Earth, Planets and Space. 2014. vol. 66. no.154 http://dx.doi.org/10.1186/s40623-014-0154-2

29. Aplin K. L., Harrison R. G. Atmospheric electric fields during the Carrington flare. Astron. Geophys. 2014. vol. 55. no. 5. pp. 5–32. http://dx.doi.org/10.1093/astrogeo/atu218

For citation: Smirnov S. E., Bychkov V. V., Mandrikova O. V., Solovev I. S., Polozov Yu. A., Zalyaev T. L., Khomutov S. Y., Baishev D. G., Poddelsky I. N., Dumbrava Z. F. Analysis of space weather events in 2014 according to the observations in the North-Eastern region of Russia. *Bulletin KRASEC. Physical and Mathematical Sciences* 2016, vol. **12**, no **1**, 58-74. DOI: 10.18454/2313-0156-2016-12-1-58-74

Original article submitted: 15.01.2016